

Measurement of the Rate Constants for the Reactions of the IO[•] Radical with Sulfur-Containing Compounds H₂S, (CH₃)₂S, and SO₂

I. K. Larin, N. A. Messineva, A. I. Spasskii, E. M. Trofimova, and L. E. Turkin

Kurchatov Institute of Atomic Energy (Troitsk Branch), Troitsk, Moscow oblast, 142092 Russia

Received October 22, 1998

Abstract—The reactions of iodine monoxide (IO[•]) with sulfur-containing compounds, which are important for the atmospheric chemistry, are studied. An attempt is made to distinguish between the heterogeneous and homogeneous reaction pathways. It is shown that, under the experimental conditions, the reactions proceed on the wall and generate iodine atoms into the gas phase. It is found that, at room temperature, the rate constants for the gas-phase reactions of IO[•] with (CH₃)₂S and H₂S are lower than 2.5×10^{-14} and 8.0×10^{-14} cm³ molecule⁻¹ s⁻¹, respectively; the rate constant for the gas-phase reaction of iodine monoxide with SO₂ $\leq 5.6 \times 10^{-15}$ cm³ molecule⁻¹ s⁻¹.

INTRODUCTION

Considerable attention has been paid to the interaction of iodine and sulfur cycles of ozone destruction during the last decade [1]. Natural sources (such as the eruption of volcanoes and biomass decomposition and combustion), as well as human activity (fuel combustion and motor engines), produce the sulfur-containing components of the atmosphere. Hydrogen sulfide and dimethylsulfide rapidly decompose in the troposphere. However, the SO₂ lifetime in the troposphere is measured in days, and about 10% of sulfur dioxide enters the stratosphere. The SO₂ concentration in the troposphere can be as high as 5×10^{11} molecule/cm³ [2]. Iodine components also have both natural (biomass decomposition) and anthropogenic sources (a growing use of iodine-containing freons) [3, 4]. Active iodine exists in the atmosphere mostly as IO[•] radicals; according to different sources, their relative concentration is $(0.1-1) \times 10^{-12}$ [5].

Several research groups have studied the reaction of iodine monoxide with dimethylsulfide using different techniques. The rate constant for the reaction was initially found to be high [6, 7]. This apparently confirmed the assumption that the reaction with IO[•] cannot account for the characteristic lifetime of dimethylsulfide. Measurements yielded a value of 15–20 min for the dimethylsulfide lifetime [6]. The lifetime of dimethylsulfide with respect to the reaction with the OH[•] radical is at least 14 hours [8].

More recently, it was found that the rate constant for the IO[•] reaction with (CH₃)₂S is much lower, namely

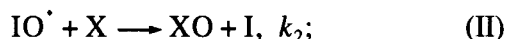
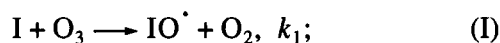
$k \leq 3.5 \times 10^{-14}$ cm³ molecule⁻¹ s⁻¹ [9], $k = (1.5 \pm 0.2) \times 10^{-14}$ cm³ molecule⁻¹ s⁻¹ [10], $k = (8.8 \pm 0.25) \times 10^{-14}$ cm³ molecule⁻¹ s⁻¹ [11]. These results ruled out the possibility for the IO[•] influence on the (CH₃)₂S lifetime in the marine atmosphere. We surmise that the high value of the rate constant reported in [6] was due to reactions on the flow reactor walls. The high value measured under static conditions by flash photolysis [7] remains unclear.

Barnes *et al.* studied the reactions of IO[•] radicals with H₂S and SO₂ studied in [12], but they did not report the rate constants. However, Barnes *et al.* affirmed that IO[•] reacted with H₂S no faster than with (CH₃)₂S, and SO₂ was the major product of the reaction (~100%). Barnes *et al.* suggested that the reaction proceeded via H-atom abstraction from hydrogen disulfide, but they did not observe HOI in the IR spectrum. IO[•] reacts with SO₂ three orders of magnitude more slowly than with dimethylsulfide.

We measured the rate constants for the iodine monoxide (IO[•]) reactions with (CH₃)₂S, H₂S, and SO₂, which produce atomic iodine. The concentration of the latter was measured by the resonance fluorescence technique. This technique allowed us to perform the measurements at active iodine concentrations lower than 3×10^{10} atom cm⁻³ and avoid the fast self-reaction of IO[•] resulting in the formation of iodine atoms.

The idea of the experiment was as follows. Atomic iodine entered the reactor in a concentration proportional to the resonance fluorescence signal. A chain

process in the reactor included two steps of the chain propagation:



where $X = (CH_3)_2S, H_2S, SO_2$.

If no additional source of atomic iodine or observable chain termination reaction of active iodine exist, the relationship between the steady-state concentrations of iodine atoms and IO^\cdot radicals is given by the expression

$$[I]_0 - [I]_{ss} = [IO^\cdot]_{ss}, \quad (1)$$

where $[I]_0, [I]_{ss}$ are the initial and steady-state concentrations of iodine atoms and $[IO^\cdot]_{ss}$ is the steady-state concentration of IO^\cdot . In the steady-state approximation,

$$k_1[I][O_3] = k_2[IO^\cdot][X], \quad (2)$$

and together with equation (1), we have

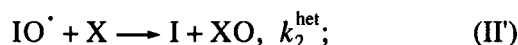
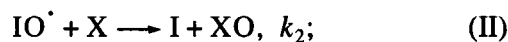
$$[I]_0/[I]_{ss} - 1 = k_1[O_3]/k_2[X]. \quad (3)$$

Measurements of the rate constant for reaction (I) reported in several papers are in good agreement. All other values except k_2 , are known from experiments. Therefore, we find the rate constant for reaction (II) k_1 from the slope of the measured J_0/J_{ss} values plotted against $[O_3]/[X]$. The measured ratio of the resonance fluorescence signals of iodine atoms J_0/J_{ss} is equal to $[I]_0/[I]_{ss}$.

Note that, if the reaction is homogeneous with no additional sink or source of atomic iodine, the experimental line intercepts the y-axis at $y = 1$. If it is not, some processes are missing in the reaction mechanism. The heterogeneous pathway of reaction (II) is one of the possible missing processes.

In flow experiments, the rate constant is usually calculated from a reagent or a reaction product concentration plotted as a function of the residence time in the reactor. The characteristic time of a reaction is generally much longer than that of the diffusion of active species to the wall. This inevitably results in the involvement of these species in both homogeneous and heterogeneous processes. In the suggested method, we find the rate constant using the steady-state concentration of the active species involved in the chain process. In this case, the characteristic time of every elementary step can be shorter than that of the diffusion of active species to the wall. This makes it possible to separate homogeneous and heterogeneous reaction pathways.

We assume that the chain process includes the following steps:



where (I) and (II) are homogeneous steps and (II') is heterogeneous. Then the rate of the atomic iodine generation is

$$w = k_2[IO^\cdot][X] + k_2^{\text{app}}[IO^\cdot], \quad (4)$$

where

$$1/k_2^{\text{app}} = 1/(k_2^{\text{het}}[X]) + 1/k_{\text{diff}},$$

$$k_{\text{diff}} = 23D/4R^2.$$

Here k_2^{app} is the apparent rate constant for the heterogeneous reaction with diffusion; $k_2^{\text{het}}[X]$ is the apparent rate constant under kinetically controlled conditions; D is the diffusion coefficient for IO^\cdot radicals; R is the radius of the reactor in centimeters. $D = D_0(760/P)$, where D_0 is the diffusion coefficient for IO^\cdot at 760 torr; P is the pressure in the reactor, torr. $D_0 = 0.12 \text{ cm}^2/\text{s}$ at $T = 296 \text{ K}$.

Then the steady-state concentration of atomic iodine is

$$k_1[I]_{ss}[O_3] = k_2[IO^\cdot]_{ss}[X] + k_2^{\text{app}}[IO^\cdot]_{ss}, \quad (5)$$

where $[I]$ and $[IO^\cdot]$ are related to $[I]_0$ by equation (1).

Using Eqs. (4), (5), and (1), we arrive at the relationship between the steady-state concentration of atomic iodine and the concentration of reagent X . The rate constant for the reagent X reaction with IO^\cdot radical is

$$[I]_0/[I]_{ss} = 1 + \frac{k_1[O_3]/[X]}{k_2 + k_2^{\text{het}}0.5k_{\text{diff}}/(k_2^{\text{het}}[X] + 0.5k_{\text{diff}})}. \quad (6)$$

The factor before k_{diff} in Eq. (6) is due to the fact that the reactor geometry differs from cylindrical near the registration zone, and the entire surface is not accessible to the active species. A value of 0.5 for the coefficient is found by fitting theoretical curves and experimental data for the well-studied reaction of IO^\cdot with dimethylsulfide.

Using Eq. (6), we can plot the ratio $[I]_0/[I]_{ss}$ versus $[O_3]/[X]$ at different ratios $k_2/(k_2 + k_2^{\text{het}})$ (different homogeneity of the reaction) and show the experimental points in the same plot. The slope of the experimental line gives the value $(k_2 + k_2^{\text{het}})$.

EXPERIMENTAL

We performed experiments under flow conditions in a cylindrical reactor (Fig. 1) at 343 K. The distance between the registration zone and the point where reagents entered through the mobile inlet is marked on Fig. 1 as L . We varied the distance from the maximal value (close to the total reactor length) to 1 cm.

A constant-temperature jacket maintained the reactor temperature at 343 K with an accuracy of 1%. The inner surface of the reactor (the inner diameter is 1.7 cm) was coated with 32-L fluoroplastics. Hydrogen sulfide and SO_2 were produced in the laboratory by reactions of Na_2S and Na_2SO_3 with sulfuric acid. Dimethylsulfide was synthesized by the reaction of methyl iodide with Na_2S [15].

We determined the concentrations of sulfur-containing compounds in the reaction vessel by measuring the time necessary for a specified amount of a compound to flow out from a calibrated volume. A pressure change was monitored by a standard pressure gauge. We used chemical purity grade oxygen and high purity grade helium in all experiments.

Ozone was produced by flowing oxygen through an Ozon-2 ozonizer. The ozone concentration was measured by a Spectromom-204 spectrometer using a change in the absorbance at $\lambda = 253.7$ nm. The following expression gives the amount of ozone entering the reactor:

$$Q_{\text{O}_3} = Q_{\text{O}_2} \frac{2.3D_{253.7}}{(273/T)3.55 \times 10^{16} \sigma l P_{\text{cell}}} \text{ cm}^3 \text{ torr s}^{-1},$$

where Q_{O_2} , Q_{O_3} are oxygen and ozone flows, respectively, $\text{cm}^3 \text{ torr s}^{-1}$; $D_{253.7}$ is the absorbance; $\sigma = 1.15 \times 10^{-17} \text{ cm}^2$ is the absorption cross section; l is the length of the optical cell; P_{cell} is the pressure in the optical cell, torr; and T is the temperature in the cell.

All pipes used to supply ozone into the reactor were made of glass and Teflon and contained no vacuum grease.

Source of atomic iodine. Iodine atoms were produced in a quartz tube with an inner diameter of ~8–10 mm connected to the reactor through a capillary (1 mm in diameter and 1 cm in length). The tube was irradiated by a quartz mercury low-pressure DRB-8 (8 W) lamp. A stabilizing power supply B-2-3 was used with a choke coil. The lamp had an opaque cover except for the operating area (4 cm length).

A mixture of helium with gaseous methyl iodide flowed through the source of iodine atoms. UV radiation ($\lambda = 253.7$ nm) produced $^2P_{1/2}$ and $^2P_{3/2}$ iodine atoms (20% of them were produced in the ground state $^2P_{3/2}$ [16]).

The deactivation of $^2P_{1/2}$ iodine atoms partially occurred on CH_3I molecules in the atom source itself and partially on oxygen molecules in the reactor. The

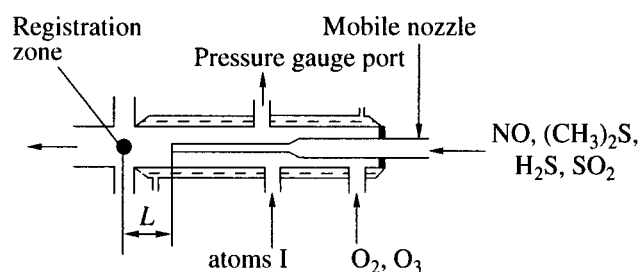


Fig. 1. Schematic of the reactor.

ampule with CH_3I (analytical grade) was kept in a melting ice bath at 0°C .

Automated system for the registration of iodine atoms. The resonance fluorescence technique for the registration of iodine atoms consisted of a resonance lamp emitting the resonance 178.3-nm line of atomic iodine, a photoionization counter detecting photons reemitted by iodine atoms, and a frequency meter ChZ-63/1 interfaced with a computer recording signals for further analysis of the data. The system was described in detail in [16, 17]. Therefore, only a brief description is given here.

Registration zone. The registration zone consisted of a photon counter, a Wood horn and, two crossed tubes (10 mm in diameter and 10 mm in length) soldered with the reactor. The tubes had quartz couplings on their ends, in which brass cones of the resonance lamp, of the photon counter, and of the Wood horn were installed in vacuum grease. Copper tubes with an inner diameter of 6 mm were inserted into the cones of the lamp and of the photon counter. The distances between the tubes and the L -zone of the reactor were 3 mm. These tubes collimated the emission of the resonance lamp and increased the heterogeneous decay of iodine atoms diffusing into the tubes of the cross.

The copper tubes and the internal surface of the cross were coated with MgO to increase the accommodation coefficient of iodine atoms.

Resonance lamp. The flow resonance lamp was made of quartz. The inner diameter of the operating zone was 3 mm. The optical windows (UV quartz) had a short-wave transparency limit of 160 nm. Indium gaskets ensured the leakproofness of the system. The collimating system was placed inside an NSh-19 brass cone connecting the lamp with the reactor. Helium containing molecular iodine (10000 : 1) was made to flow through the lamp. A metallic bellows pressure gauge monitored pressure in the lamp with an accuracy of 0.01 torr. The gas flow rate through the lamp was ~3500 cm/s.

A Broida microwave resonator was used to activate a microwave discharge. A LUCH-3M microwave generator with an output power of 2.5 W was used as a source of microwave energy.

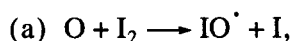
Photoionization counter A photoionization counter was used to detect reemitted photons. The tungsten filament of the counter (0.3 mm in diameter) was soldered with a glass beaker. Through a dividing capacitor ($C = 470$ pF), the signal simultaneously traveled to a ChZ-63/1 frequency meter and an S-107 oscilloscope. The frequency meter combined with the computer accumulated from 500 to 10^4 pulses in each experimental point. The oscilloscope was used in the waiting mode to control the amplitude of impulses and the dead time of the system. The end window of the counter was made of UV quartz with a short-wave transparency limit of ~ 160 nm. The brass NSh-19 body connected the counter to the reactor. The collimating system with a diaphragm was assembled inside the cone.

After having evacuated the counter to a pressure of 5×10^{-5} torr with a diffusion pump, we filled it up with a mixture of NO (10 torr) and Ar (230 torr). A drop of diethylferrocene in a glass finger equalized the vapor pressure. The long-wave threshold of the counter was determined by the ionization energy of diethylferrocene (6.3 eV) and had a value of ~ 185 nm.

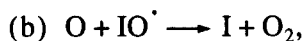
Thus, the photoionization counter worked also as a monochromator and isolated the spectral range from ~ 160 to 185 nm.

Calibration of the absolute sensitivity of the setup to iodine atoms. It was necessary to create some known concentration of iodine atoms in the reactor to calibrate the sensitivity of the system. To avoid spurious signals, a very small amount of molecular iodine was present in the reactor.

Molecular iodine in excess oxygen atoms produced a known amount of iodine atoms. The following reactions occurred in the system:



$$k_a = 1.38 \times 10^{-10} \text{ cm}^3 \text{ molecule}^{-1} \text{ s}^{-1} [18];$$



$$k_b = 5 \times 10^{-11} \text{ cm}^3 \text{ molecule}^{-1} \text{ s}^{-1} [19];$$



Oxygen atoms were generated in a microwave discharge in the 4% $\text{O}_2 + \text{He}$ mixture.

We used the chemiluminescent titration with NO_2 to estimate the concentration of oxygen atoms. This concentration ($\sim 10^{14}$ atom/cm³) exceeded the iodine atom concentration by three orders of magnitude. Therefore, the heterogeneous decay of oxygen atoms was the major channel of their consumption.

Therefore, the source of atomic iodine enabled us to produce a known amount of iodine atoms and transport them to the distance controlled by the heterogeneous

decay of atomic oxygen. The concentration of atomic iodine was virtually invariable.

Under our experimental conditions, the signal-to-noise ratio was equal to unity at an iodine atom concentration of $\sim 3 \times 10^7$ atom/cm³.

The reactions of dimethyl sulfide and hydrogen sulfide with ozone resulted in the deposition of reaction products on the optical windows. This changed the resonance fluorescence signal and complicated the study of these reactions. To avoid the deposition of products in the areas close to the optical windows, a helium flow was directed to the windows of the resonance fluorescence source and the photoionization counter.

It is known that the rate constants for the ozone reactions with $(\text{CH}_3)_2\text{S}$, H_2S , and SO_2 are low [20]. However, under some conditions, these reactions can proceed via a complex chain mechanism. In our experiments, a bright flash followed the mixing of both hydrogen sulfide and dimethylsulfide with ozone at ~ 1 torr. The spectrum of the flash was similar to that of the excited SO_2 molecule. The absorption spectrum of ozone at 253.7 nm disappeared for a time shorter than 1 s. Thus, it is necessary to monitor the level of reagent conversion during the study of the IO^\cdot reaction with $(\text{CH}_3)_2\text{S}$, H_2S , and SO_2 .

$(\text{CH}_3)_2\text{S}$, H_2S , and SO_2 entered the reactor through a mobile nozzle with an outer diameter of 3 mm covered with fluoroplastic 32-L and positioned at a known distance from the registration zone. The distance was small enough to minimize the consumption of reagents or ozone but sufficient for achieving the steady-state concentration of iodine atoms. The distance of 3 cm gave the contact time equal to 9×10^{-3} s; the characteristic time necessary for the steady-state concentration of iodine atoms was shorter than 1×10^{-3} s. This ratio of the contact time and the characteristic time enabled us to carry out measurements at the steady-state concentration of iodine atoms.

RESULTS AND DISCUSSION

Reaction $\text{IO}^\cdot + \text{NO}$

We tested the above technique on the reaction of IO^\cdot radicals with nitric oxide previously studied by us:



The dependence of J_0/J on $[\text{O}_3]/[\text{NO}]$ was obtained at $T = 343$ K. NO entered the reactor at a fixed distance of 3 cm from the registration zone. J_0 is the signal of iodine atoms when no ozone was present in the reactor; J is the same signal with O_3 and NO entering the reactor; $[\text{O}_3]$ and $[\text{NO}]$ are ozone and nitric oxide concentrations corrected for the burn-up of reagents during their reactions with each other.

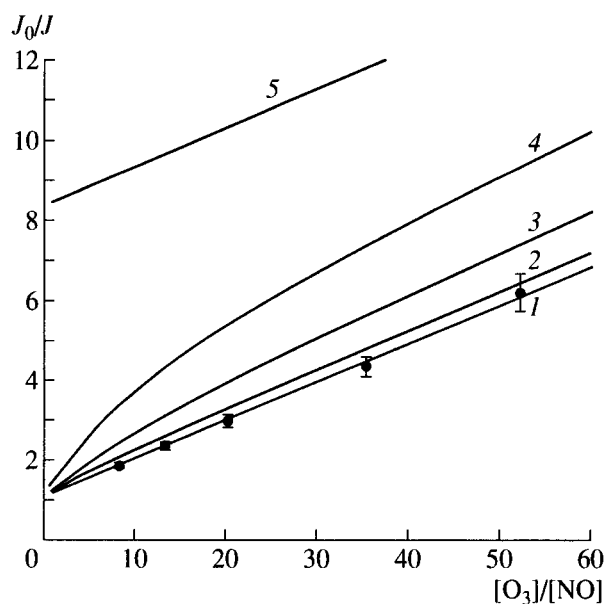
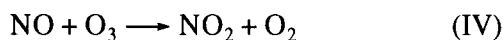


Fig. 2. A plot of J_0/J versus $[O_3]/[NO]$ at $L = 3$ cm, $T = 343$ K. The dots correspond to the experimental data. The solid lines were calculated using equation (6) for the degree of reaction homogeneity ($k_3/(k_3 + k_3^{\text{het}})$) equal to 1.0 (1), 0.75 (2), 0.5 (3), 0.25 (4), and 0 (5).

The rate constant for the reaction



was taken from the published data [14].

Figure 2 shows the results of the experiment (dots) and the results calculated using equation (6) for various degrees of homogeneity of the reaction $k_2/(k_3 + k_3^{\text{het}})$.

As seen from Fig. 2, reaction (III) occurs in the gas phase. The slope of the experimental straight line gives a value of $1.85 \times 10^{-11} \text{ cm}^3 \text{ molecule}^{-1} \text{ s}^{-1}$ for this rate constant. This value coincides with that measured in [14]. The length of the contact zone (3 cm) and corresponding contact time $\tau \sim 9 \times 10^{-3} \text{ s}$ sufficed for the steady-state concentration of iodine.

Reactions $\text{IO}^\bullet + (\text{CH}_3)_2\text{S}$, $\text{IO}^\bullet + \text{H}_2\text{S}$ and $\text{IO}^\bullet + \text{SO}_2$

We used the setup shown in Fig. 1 to study the reactions $\text{IO}^\bullet + (\text{CH}_3)_2\text{S}$, $\text{IO}^\bullet + \text{H}_2\text{S}$, and $\text{IO}^\bullet + \text{SO}_2$. These reagents, when added to the flow containing O_2 and O_3 , produced iodine atoms. Additional experiments showed that $(\text{CH}_3)_2\text{S}$, H_2S , SO_2 , and the products of their reactions sharply increased the rate of the IO^\bullet heterogeneous decay at temperatures below 320 K. So we performed the experiments at 343 K. Figure 3 shows the value of J_0/J plotted against $[O_3]/[(\text{CH}_3)_2\text{S}]$, $[O_3]/[\text{H}_2\text{S}]$, and $[O_3]/[\text{SO}_2]$. The dots correspond to the experimental data; the solid lines were calculated using

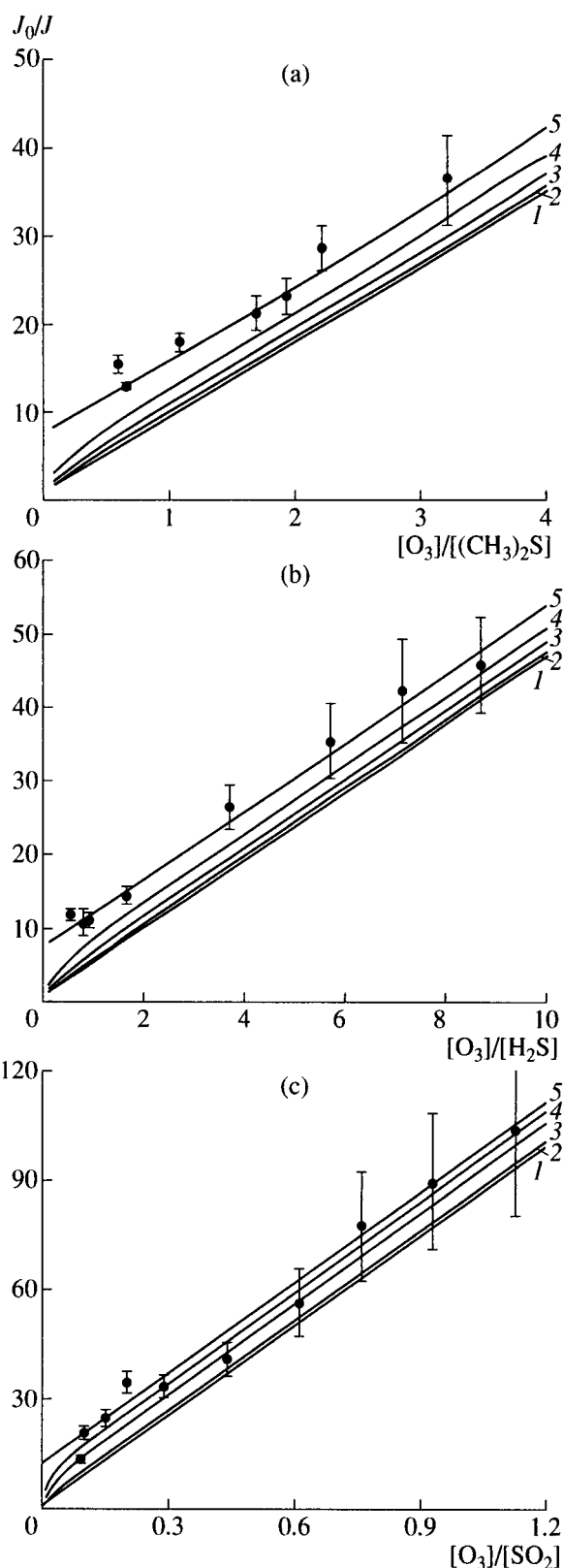


Fig. 3. A plot of J_0/J versus $[O_3]/[X]$ at $L = 3$ cm, $T = 343$ K. The dots correspond to the experimental data. The solid lines were calculated using equation (6) for the degree of reaction homogeneity ($k_2/(k_2 + k_2^{\text{het}})$) equal to 1.0 (1), 0.75 (2), 0.5 (3), 0.25 (4), and 0 (5): X = $(\text{CH}_3)_2\text{S}$ (a), H_2S (b), and SO_2 (c).

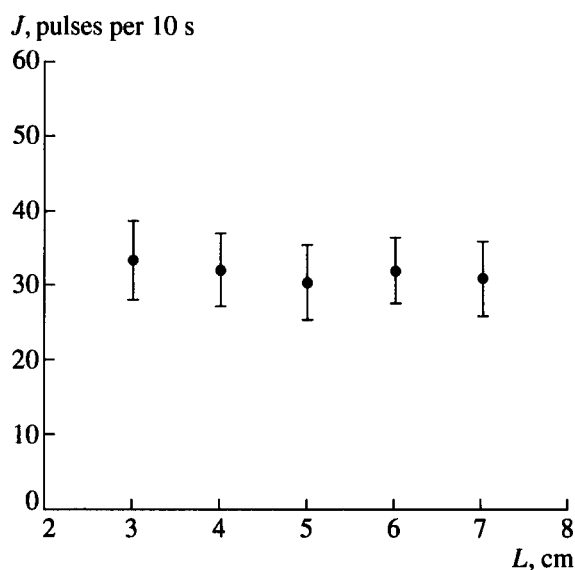


Fig. 4. The signal of the resonance fluorescence J versus the distance between the inlet of $(\text{CH}_3)_2\text{S}$ and the iodine atoms registration zone. $T = 343$ K.

equation (6) and the degree of homogeneity of the reaction varied from 0 to 1. The apparent rate constants k_2^{app} equal to the sum of the homogeneous and the heterogeneous rate constants were:

for $(\text{CH}_3)_2\text{S}$,

$$k_2^{\text{app}} = (2.0 \pm 0.5) \times 10^{-13} \text{ cm}^3 \text{ molecule}^{-1} \text{ s}^{-1};$$

for H_2S ,

$$k_2^{\text{app}} = (3.8 \pm 0.2) \times 10^{-13} \text{ cm}^3 \text{ molecule}^{-1} \text{ s}^{-1};$$

for SO_2 ,

$$k_2^{\text{app}} = (2.1 \pm 0.7) \times 10^{-14} \text{ cm}^3 \text{ molecule}^{-1} \text{ s}^{-1};$$

Then, it became possible to estimate the homogeneous rate constants for these reactions as

$$k_2^{(\text{CH}_3)_2\text{S}} \leq (0.0 - 0.1) k_2^{\text{app}},$$

$$k_2^{\text{H}_2\text{S}} \leq (0.1 - 0.2) k_2^{\text{app}},$$

$$k_2^{\text{SO}_2} \leq (0.1 - 0.2) k_2^{\text{app}}$$

or

$$k_2^{(\text{CH}_3)_2\text{S}} \leq 2.5 \times 10^{-14} \text{ cm}^3 \text{ molecule}^{-1} \text{ s}^{-1},$$

$$k_2^{\text{H}_2\text{S}} \leq 8 \times 10^{-14} \text{ cm}^3 \text{ molecule}^{-1} \text{ s}^{-1},$$

$$k_2^{\text{SO}_2} \leq 5.6 \times 10^{-15} \text{ cm}^3 \text{ molecule}^{-1} \text{ s}^{-1}.$$

A chain reaction of ozone with dimethylsulfide, hydrogen sulfide, and SO_2 can occur in the system and result in the burn-up of reagents. To make sure that the burn-up did not happen, we studied the dependence of the resonance fluorescence signal on the distance between the registration zone and the reagents inlet at constant concentrations of ozone, dimethylsulfide, hydrogen sulfide, and sulfur dioxide. The quasi-steady-state concentration of iodine atoms depended only on the initial concentration of IO^\cdot radicals and $[\text{O}_3]/[\text{X}]$, where $[\text{X}] = (\text{CH}_3)_2\text{S}$, H_2S , and SO_2 . The resonance fluorescence signal was independent of the ozone contact time with $(\text{CH}_3)_2\text{S}$, H_2S , and SO_2 . This demonstrated that the ratio $[\text{O}_3]/[\text{X}]$ did not change and no burn-up of reagents occurred. Figure 4 shows a plot of the signal intensity J (the resonance fluorescence signal) versus the distance between the nozzle and the registration zone L . Within the error limits ($\leq 12\%$ for dimethylsulfide), the resonance fluorescence signal did not change with a change in the contact time in the case of ozone and $(\text{CH}_3)_2\text{S}$. For H_2S and SO_2 the signal was invariable within $\sim 10\%$.

ACKNOWLEDGMENTS

This work was supported by the Russian Foundation for Basic Research, project no. 96-0565477.

REFERENCES

1. Chatfield, R.B. and Crutzen, P.J., *J. Geophys. Res.*, 1990, vol. 95, no. 11, p. 22 319.
2. Brassier, G. and Solomon, S., *Aeronomiya srednei atmosfery* (Aeronomy of the Middle Atmosphere), Leningrad: Gidrometeoizdat, 1987, p. 283.
3. Chameides, W.L. and Davis, D.D., *J. Geophys. Res.*, 1980, vol. 85, no. 12, p. 7383.
4. Jenkin, M.E., Cox, R.A., and Candeland, D.E., *J. Atmos. Chem.*, 1985, vol. 2, no. 1, p. 353.
5. Pundt, I., Philips, C., and Pommereau, J.P., *Proc. XVIII Symp. on the Atmospheric Ozone*, Aquila, 1996.
6. Martin, D., Jourdain, J.L., Laverdet, G., and Le Bras, G., *Int. J. Chem. Kinet.*, 1987, vol. 19, no. 2, p. 503.
7. Barnes, J., Becker, K.H., Carlier, P., and Mouvier, G., *Int. J. Chem. Kinet.*, 1987, vol. 19, no. 2, p. 487.
8. Atkinson, R., Baulch, D.L., Cox, R.A., *et al.*, *J. Phys. Chem. Ref. Data*, 1992, vol. 21, p. 1125.
9. Daykin, E.P. and Wine, P.H., *J. Geophys. Res.*, 1990, vol. 95, p. 1848.
10. Marguin, F.O., Mellouki, A., Laverdet, G., *et al.*, *Int. J. Chem. Kinet.*, 1992, vol. 23, no. 1, p. 237.
11. Barnes, J., Bastian, V., Becker, K.H., and Overath, R.D., *Int. J. Chem. Kinet.*, 1991, vol. 23, no. 2, p. 579.

12. Barnes, J., Bastian, V., and Becker, K.H., *Air Pollution Research Report OCEANO-NOX Project*, Restelli, G., Ed., Dordrecht: Kluwer Academic, 1990, p. 166.
13. Sander Stanley, P., *J. Phys. Chem.*, 1986, vol. 90, p. 2194.
14. Buben, S.N., Larin, I.K., Messineva, N.A., and Trofimova, E.M., *Khim. Fiz.*, 1996, vol. 15, no. 1, p. 116.
15. McAllen, D.T., Gullum, T.V., Dean, R.A., and Fidler, F.A., *J. Am. Chem. Soc.*, 1951, vol. 73, p. 3626.
16. Buben, S.N., Larin, I.K., Messineva, N.A., and Trofimova, E.M., *Khim. Fiz.*, 1990, vol. 8, no. 9, p. 1234.
17. Buben, S.N., Larin, I.K., Messineva, N.A., and Trofimova, E.M., *Khim. Fiz.*, 1990, vol. 9, no. 1, p. 116.
18. Ray, C.W. and Watson, R.J., *J. Phys. Chem.*, vol. 85, p. 1955.
19. Baulch, D.L., Cox, R.A., Crutzen, P.J., *et al.*, *CODATA*, 1982, no. 6, p. 337.
20. De More, W.B., Sander, S.P., Golden, D.M., *et al.*, *Chemical Kinetics and Photochemical Data for Use in Stratospheric Modeling*, Pasadena: JPL 97-4, 1997, p. 1.